Synthesis and Crystal Structures of $[W(3,6\text{-dichloro-1,2-benzenedithiolate})_3]^{n-}$ (n = 1, 2) and $[Mo(3,6\text{-dichloro-1,2-benzenedithiolate})_3]^{2-}$: Dependence of the Coordination Geometry on the Oxidation Number and Counter-Cation in Trigonal-Prismatic and Octahedral Structures

Hideki Sugimoto,*[a] Yuuki Furukawa,[a] Makoto Tarumizu,[a] Hiroyuki Miyake,[a] Koji Tanaka,[b] and Hiroshi Tsukube[a]

Keywords: Coordination modes / Molybdenum / S ligands / Salt effects / Tungsten

The novel complexes $(Et_4N)_2[W(bdtCl_2)_3]$ (**1a**), $(Ph_4P)_2[W(bdtCl_2)_3]$ (**1b**), $(Et_4N)[W(bdtCl_2)_3]$ (**2a**), $(Ph_4P)[W(bdtCl_2)_3]$ (**2b**), $(C_5NH_6)[W(bdtCl_2)_3]$ (**2c**), and $(Et_3NH)_2[Mo(bdtCl_2)_3]$ (**3a**) ($bdtCl_2$ = 3,6-dichloro-1,2-benzenedithiolate) were prepared and characterized by X-ray crystallographic, UV/Vis spectroscopic, and electrochemical methods. Versatile geometrical changes around the tungsten centers were observed. The trigonal-prismatic structure of the tungsten center in $(Et_4N)_2[W(bdtCl_2)_3]$ (**1a**) is changed to an intermediate structure between trigonal prismatic and octahedral upon solid-state oxidation of the complex to $(Et_4N)[W(bdtCl_2)_3]$ (**2a**). Replacement of the counter-cation of $(Et_4N)_2[W(bdtCl_2)_3]$ (**1a**) with Ph_4P^+ also resulted in geometrical changes and somewhat of an octahedral contribution is included in $(Ph_4P)_2[W(bdtCl_2)_3]$ (**1b**). However, almost the same coordination structures are present in the series of structures $(Et_4N)[W(bdtCl_2)_3]$ (**2a**), $(Ph_4P)[W(bdtCl_2)_3]$ (**2b**), and $(C_5NH_6)[W(bdtCl_2)_3]$ (**2c**), with an oxidation number of +5. These structures adopt an intermediate geometry between trigonal prismatic and octahedral. No geometrical change was observed upon changing the metal center from tungsten to molybdenum in $[M(bdtCl_2)_3]^{2-}$ (M = W and Mo).

Introduction

In recent years, much attention has been directed toward the synthesis of metal complexes containing dithiolene ligands. This interest is primarily due to their utility in magnetic materials, superconductors, nonlinear optical materials, luminescent sensors, and enzyme catalytic centers.[1–4] The synthetic routes to tungsten and molybdenum complexes with dithiolene ligands have been extensively developed,[5,6] and their tris(dithiolene) complexes have been well characterized.[7] These tris(dithiolene) complexes show interesting characteristics in terms of both reversible electron-transfer reactions and geometrical variations around the metal centers. Although six-coordinate metal complexes generally exhibit an octahedral coordination geometry to minimize ligand interactions, it is well known that tris(dithiolene) complexes of molybdenum and tungsten can adopt both octahedral (OCT) and trigonal-prismatic (TP) structures (Scheme S1 in the Supporting Information).[7]

According to the classification of Beswick et al., the coordination geometries are found to largely depend on the nature of the coordinated dithiolene ligands.[7] $[M(mnt)_3]^{2-}$ (M = W and Mo; mnt = 1,2-dicyano-1,2-ethylenedithiolate) complexes[8] adopt intermediate structures between OCT and TP [OCT/TP = average of the values for θ/60 and (90 – φ)/(90 – 55) = 53% for M = Mo and W],[7] whereas $[M(S_2C_2Me_2)_3]^{2-}$ (M = W and Mo; $S_2C_2Me_2$ = 1,2-dimethylethylene-1,2-dithiolate) complexes[9] primarily adopt TP structures (OCT/TP = 1% for M = W and 2% for Mo).[7] When the bdt ligand is employed (bdt = benzene-1,2-dithiolate), $[W(bdt)_3]^{2-}$ structures largely depend on these counter-cations. The $(Ph_4As)_2[W(bdt)_3]$ structure[10] is intermediate between TP and OCT (OCT/TP = 44%),[7] whereas $(Et_4N)_2[W(bdt)_3]$[11] adopts a TP structure (OCT/TP = 2%).[7] The oxidation numbers of the metal centers also have an effect on the geometries. Examples of structurally characterized M^{IV}, M^{V}, and M^{VI} complexes with the same dithiolene ligands and counter-cations are limited to $(Et_4N)_n[M(S_2C_2Me_2)_3]^{0/-/2-}$ (M = W and Mo, n = 0, 1, and 2),[9,12] but all the six complexes adopt near TP geometries.[7] On the other hand, $[W(bdt)_3]^{0/-/2-}$ [10–14] and $[W(S_2C_2Ph_2)_3]^{0/-}$ ($S_2C_2Ph_2$ = 1,2-phenylethylene-1,2-dithiolate)[15] structures adopt variable geometries ranging from OCT/TP = 0% to OCT/TP = 62% (former), and from 39% to 2% (latter).[7] Because these complexes have different

[a] Department of Chemistry, Graduate School of Science, Osaka City University,
Sumiyoshi-ku 3-3-138, Osaka 558-8585, Japan
Fax: +81-6-6605-2522
E-mail: sugimoto@sci.osaka-cu.ac.jp
[b] Institute for Molecular Science,
Higashiyama, Okazaki, 444–8787, Japan
Supporting information for this article is available on the WWW under http://www.eurjic.org or from the author.

  DOI: 10.1002/ejic.200500074

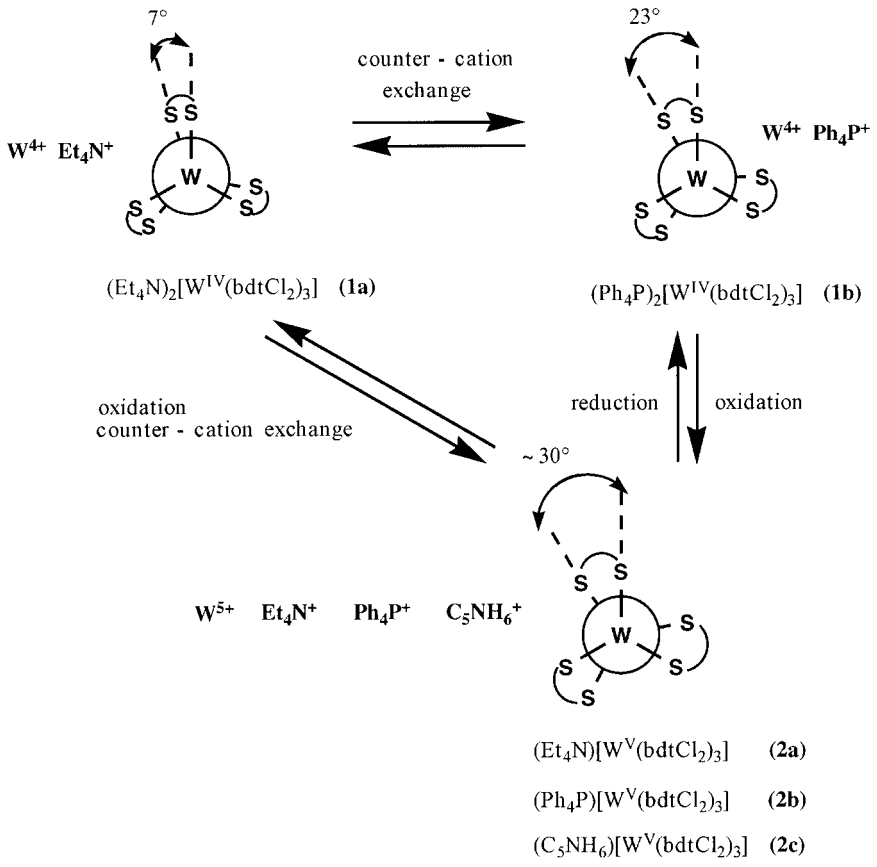

Scheme 1. Diagram showing geometrical changes.

counter-cations, including $Me_2Ph_2P^+$, Me_4N^+, Et_4N^+, Ph_4As^+, and $PhCH_2(Et)_3N^+$, and the effects of the oxidation number and counter-cation on the geometry still remain unclear, we have systematically characterized a series of $[M(dithiolene)_3]^{-/2-}$ (M = W and Mo) complexes containing the same counter-cations but weaker electron-donating dithiolene ligands than $S_2C_2Me_2$. The structural comparison between the tris($bdtCl_2$) complexes of tungsten and molybdenum ($bdtCl_2$ = 3,6-dichloro-1,2-benzenedithiolate) $(Et_4N)_2[W(bdtCl_2)_3]$ (**1a**), $(Ph_4P)_2[W(bdtCl_2)_3]$ (**1b**), $(Et_4N)[W(bdtCl_2)_3]$ (**2a**), $(Ph_4P)[W(bdtCl_2)_3]$ (**2b**), $(C_5NH_6)[W(bdtCl_2)_3]$ (**2c**), and $(Et_3HN)_2[Mo(bdtCl_2)_3]$ (**3a**) reveals new insights into the factors governing the structures of tris(dithiolene) complexes (Scheme 1).

Results and Discussion

Structural Characterization

Figures 1, 2, and 3 show the crystal structures of the anionic tungsten(IV) complexes **1a** and **1b**, and the molybdenum(IV) complex **3a**, respectively, and Figures 4, 5, and 6 show those of the tungsten(V) complexes **2a**–**2c**, respectively. The metal centers of all anions are coordinated to six sulfur atoms from three $bdtCl_2$ ligands, and all the anions interact with the counter-cations through C–H···S bonds (3–3.6 Å). The crystal structure of **2c** reveals that the pyridinium cation stacks between the aromatic phenyls of two anions (ca. 3.5 Å) to form a chain structure (not shown). The θ and φ values (see Experimental Section) given in Scheme S1 are good indications for a geometry between TP (θ = 0° and φ = 90°) and OCT (θ = 60° and $\varphi \approx$ 55°). The values of our new complexes and related complexes taken from the literature are listed in Table 1.

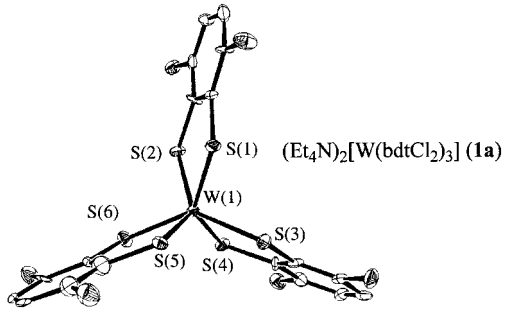

Figure 1. Structure of anion part of **1a** with 50% probability thermal ellipsoids. Selected bond lengths [Å] and angles [°]: W(1)–S(1) 2.374(5), W(1)–S(2) 2.381(5), W(1)–S(3) 2.382(4), W(1)–S(4) 2.358(5), W(1)–S(5) 2.372(4), W(1)–S(6), 2.378(5); S(2)–W(1)–S(1) 81.2(2), S(4)–W(1)–S(1) 141.3(2), S(6)–W(1)–S(1) 131.1(2), S(3)–W(1)–S(2) 128.4(2), S(4)–W(1)–S(2) 82.9(2), S(5)–W(1)–S(2) 139.5(2),S(4)–W(1)–S(3) 81.4(2), S(6)–W(1)–S(3) 141.2(2), S(5)–W(1)–S(4) 130.6(2), S(6)–W(1)–S(5) 81.3(2).

The tungsten(IV) center in **1a** adopts an almost TP structure (θ = 7°, φ = 86°, and OCT/TP = 12%; Scheme S1).

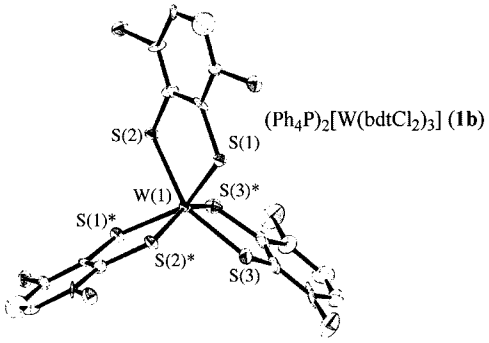

Figure 2. Structures of anion part of **1b** with 50% probability thermal ellipsoids. Selected bond lengths [Å] and angles [°]: W(1)–S(1) 2.380(1), W(1)–S(2) 2.393(1), W(1)–S(3) 2.379(2); S(1)–W(1)–S(1)* 150.63(6), S(2)–W(1)–S(1) 82.62(4), S(3)*–W(1)–S(1) 119.00(5), S(3)*–W(1)–S(2) 153.02(5), S(3)–W(1)–S(2)* 153.02(5), S(3)*–W(1)–S(3) 82.01(6).

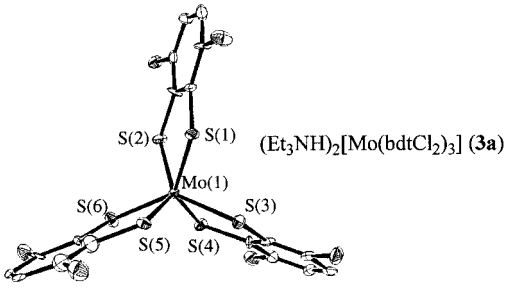

Figure 3. Structure of anion part of **3a** with 50% probability thermal ellipsoids. Selected bond lengths [Å] and angles [°]: Mo(1)–S(1) 2.383(5), Mo(1)–S(2) 2.384(4), Mo(1)–S(3) 2.394(4), Mo(1)–S(4) 2.380(5),Mo(1)–S(5) 2.409(4), Mo(1)–S(6), 2.378(5); S(2)–Mo(1)–S(1) 81.7(2), S(4)–Mo(1)–S(1) 131.7(2), S(6)–Mo(1)–S(1) 136.7(2), S(3)–Mo(1)–S(2) 137.1(2), S(4)–Mo(1)–S(2) 81.7(2), S(5)–Mo(1)–S(2) 134.4(2),S(4)–Mo(1)–S(3) 80.5(2), S(6)–Mo(1)–S(3) 133.6(2), S(5)–Mo(1)–S(4) 137.8(2), S(6)–Mo(1)–S(5) 80.2(2).

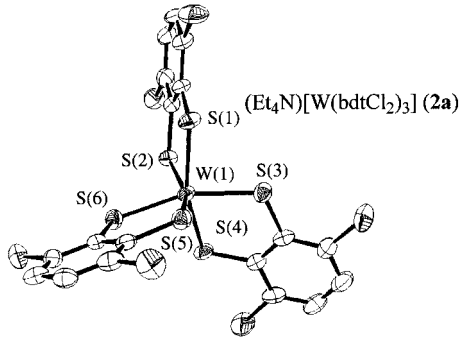

Figure 4. Structure of anion part of **2a** with 50% probability thermal ellipsoids. Selected bond lengths [Å] and angles [°]: W(1)–S(1) 2.369(3), W(1)–S(2) 2.382(3), W(1)–S(3) 2.382(3), W(1)–S(4) 2.382(3), W(1)–S(5) 2.390(3), W(1)–S(6), 2.382(3); S(2)–W(1)–S(1) 82.69(9), S(4)–W(1)–S(1) 110.7(1), S(6)–W(1)–S(1) 157.6(1), S(3)–W(1)–S(2) 159.0(1), S(4)–W(1)–S(2) 84.51(9), S(5)–W(1)–S(2) 111.8(1),S(4)–W(1)–S(3) 82.38(9), S(6)–W(1)–S(3) 109.6(1), S(5)–W(1)–S(4)160.0(1), S(6)–W(1)–S(5) 82.5(1).

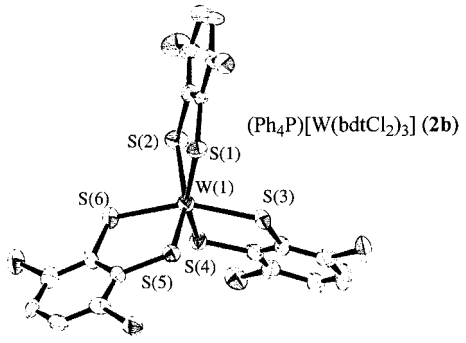

Figure 5. Structure of anion part of **2b** with 50% probability thermal ellipsoids. Selected bond lengths [Å] and angles [°]: W(1)–S(1) 2.389(3), W(1)–S(2) 2.367(2), W(1)–S(3) 2.382(2), W(1)–S(4) 2.382(2), W(1)–S(5) 2.366(2), W(1)–S(6), 2.391(2); S(2)–W(1)–S(1) 82.29(9), S(4)–W(1)–S(1) 111.27(9), S(6)–W(1)–S(1) 154.75(9), S(3)–W(1)–S(2) 155.6(1), S(4)–W(1)–S(2) 82.26(9), S(5)–W(1)–S(2) 114.62(9), S(4)–W(1)–S(3) 82.67(8), S(6)–W(1)–S(3) 113.16(9), S(5)–W(1)–S(4) 155.62(8), S(6)–W(1)–S(5) 85.12(8).

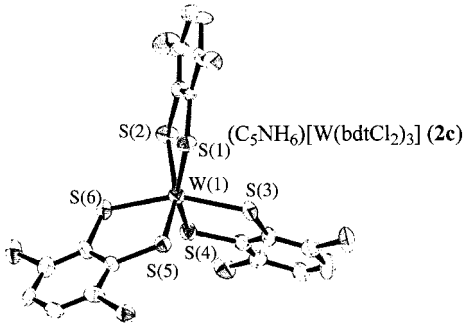

Figure 6. Structure of anion part of **2c** with 50% probability thermal ellipsoids. Selected bond lengths [Å] and angles [°]: W(1)–S(1) 2.385(3), W(1)–S(2) 2.385(3), W(1)–S(3) 2.378(3), W(1)–S(4) 2.379(3), W(1)–S(5) 2.388(3), W(1)–S(6), 2.375(3); S(2)–W(1)–S(1) 82.3(1), S(4)–W(1)–S(1) 114.4(1), S(6)–W(1)–S(1) 157.0(1), S(3)–W(1)–S(2) 157.6(1), S(4)–W(1)–S(2) 84.9(1), S(5)–W(1)–S(2) 110.6(1), S(4)–W(1)–S(3) 82.3(1), S(6)–W(1)–S(3) 111.9(1), S(5)–W(1)–S(4) 157.0(1), S(6)–W(1)–S(5) 81.8(1).

Table 1. Comparison of θ [°], φ [°], and OCT/Tp [%][a] values of **1a**, **1b**, **2a**–**2c**, **3a**, and related complexes.

	θ	φ	OCT/Tp[a]	Ref.
Trigonal prism	0	90	0	
Octahedral	60	≈55	100	
$(Et_4N)_2[W(bdtCl_2)_3]$ (**1a**)	7	86	12	[b]
$(Ph_4P)_2[W(bdtCl_2)_3]$ (**1b**)	23	76	39	[b]
$(Et_4N)[W(bdtCl_2)_3]$ (**2a**)	33	70	56	[b]
$(Ph_4P)[W(bdtCl_2)_3]$ (**2b**)	27	73	45	[b]
$(C_5NH_6)[W(bdtCl_2)_3]$ (**2c**)	30	72	50	[b]
$(Et_3NH)_2[Mo(bdtCl_2)_3]$ (**3a**)	2	88	5	[b]
$(Et_4N)_2[W(bdt)_3]$	4	87	2	[7,11]
$(Ph_4As)_2[W(bdt)_3]$	23	76	44	[7,10]
$(Me_2Ph_2P)[W(bdt)_3]$	30	72	62	[7,13]
$(Ph_4As)_2[W(mnt)_3]$	28	73	53	[7,8]

[a] Average of the values for θ/60 and $(90 - \varphi)/(90 - 55)$. [b] This work.

Interestingly, the coordination geometry of TP changes to an intermediate structure between TP and OCT upon replacing the Et_4N^+ cations of **1a** with the larger Ph_4P^+ cations in **1b** (θ = 23°, φ = 76°, and OCT/TP = 39%), despite the two metal centers having the same oxidation number. Similar geometrical changes were observed between $(Et_4N)_2[W(bdt)_3]$[11] (θ = 4°, φ = 87°, and OCT/TP = 2%)[7] and $(Ph_4As)_2[W(bdt)_3]$[10] (θ = 23°, φ = 76°, and OCT/

TP = 44%).[7] In both series of $bdtCl_2$ and bdt complexes the smaller counter-cation favors a near TP structure, whereas the larger counter-cation results in an intermediate structure between TP and OCT. Furthermore, when the tungsten(IV) is oxidized (see **1a** vs. **2a**) the coordination geometry changes considerably from an almost TP structure to an intermediate structure between TP and OCT (θ = 33°, φ = 70°, and OCT/TP = 56%). However, in complexes having the larger PPh_4^+ cation, oxidation from **1b** to **2b** (θ = 27°, φ = 73°, and OCT/TP = 45%) results in only slight changes in the coordination geometry.

The θ and φ values of **2c** (θ = 30°, φ = 72°, and OCT/TP = 50%) are similar to those for **2a** and **2b**, indicating that, in tungsten(V) $bdtCl_2$ complexes, geometrical changes rarely occur upon changing the counter-cations. Although $(Me_2Ph_2P)[W(bdt)_3]$[13] was found to adopt an intermediate structure between TP and OCT (θ = 30°, φ = 72°, and OCT/TP = 62%),[7] the structures of $(Me_2Ph_2P)_2[W(bdt)_3]$ and $[W(bdt)_3]^-$, which have different counter-cations from $Me_2Ph_2P^+$, have not been reported. The present results indicate that counter-cations significantly influence the coordination geometries in tungsten(IV) complexes, while little effect is observed in tungsten(V) complexes. Further, the geometries of complexes with small cations such as Et_4N^+ are sensitive to the oxidation state of the metal. The factors governing those geometrical changes have not been identified at this stage, but both packing forces in the crystals and matching of ligand orbitals and metal d orbitals in energies may be important for this series of tungsten $bdtCl_2$ complexes. The molybdenum center in **3a** takes an almost TP structure (θ = 2°, φ = 88°, and OCT/TP = 5%), suggesting that replacement of tungsten with molybdenum in $[M(bdtCl_2)_3]^{2-}$ complexes does not influence the coordination geometry around the metal centers.

Conclusions

A series of tungsten(IV) and -(V) tris(3,6-dichloro-1,2-benzenedithiolate) complexes with Et_4N^+, Ph_4P^+, and pyridinium cations as well as a molybdenum(IV) derivative with an Et_4N^+ cation have been presented. Solid-state crystallographic analysis reveals that the coordination geometries of the six-coordinate tungsten(IV) centers depend significantly on the sizes of the counter-cations, with a trigonal-prismatic geometry for the smaller Et_4N^+ (**1a**) and an intermediate structure between a trigonal prism and an octahedral geometry for the larger Ph_4P^+ (**1b**). On the other hand, tungsten(V) complexes including Et_4N^+, Ph_4P^+, and pyridinium cations (**2a**–**2c**) adopt almost the same intermediate structures. Furthermore, the coordination geometries around tungsten in Et_4N^+ complexes are dependent on the oxidation state of the metal (trigonal prism for W^{IV} and intermediate for W^{V}), except in the case of Ph_4P^+ complexes.

Experimental Section

$(Et_4N)_2[W(bdtCl_2)_3]$ (1a) and $(Et_4N)[W(bdtCl_2)_3]$ (2a): A CH_3CN solution (10 mL) containing H_2bdtCl_2 (0.50 g, 0.0025 mol) and Et_3N (0.75 mL, 0.0047 mol) was added slowly to a suspension of $[WOCl_3(THF)_2]$ (0.45 g, 0.001 mol) in CH_3CN (10 mL) at –40 °C. The solution was warmed to room temperature and stirred for 30 min. The obtained purple suspension was filtered and the filtrate was concentrated to about 6 mL. Addition of Et_4NI (0.38 g, 0.0015 mol) in CH_3OH (15 mL) to the solution gave a purple precipitate. The purple solid was dissolved in the minimum amount of acetone and purified by passing through an alumina column using acetone/CH_3OH as the eluent. A red component of $(Et_4N)_2[W(bdtCl_2)_3]$ was eluted first and then a purple component of $(Et_4N)[W(bdtCl_2)_3]$ was separated. Each solution was evaporated to dryness.

1a: Yield: 0.38 g (35%). $C_{34}H_{46}Cl_6N_2S_6W$ (1071.7): calcd. C 38.11, H 4.33, N 2.61. found C 37.76, H 4.08, N 2.56. UV/Vis (CH_3CN): λ_{max} (ε) = 470 nm (8300 $M^{-1}cm^{-1}$), 535 (4700).

2a: Yield 0.14 g (15%). $C_{26}H_{26}Cl_6NS_6W$ (941.46): calcd. C 33.17, H 2.78, N 1.49; found C 33.41, H 2.70, N 1.54. UV/Vis (CH_3CN): λ_{max} (ε) = 360 nm (9400 $M^{-1}cm^{-1}$), 540 (5200), 650 (sh). ESI-MS: m/z = 811.5 $[M]^-$. CV (V vs. SCE in CH_3CN): –0.19 (reversible), +0.47 (reversible).

$(Ph_4P)_2[W(bdtCl_2)_3]$ (1b): The complex was prepared in the same way as **1a** except that PPh_4Br was employed instead of Et_4NI. Yield: 0.58 g (39%). $C_{66}H_{46}Cl_6P_2S_6W$ (1490.0): calcd. C 53.20, H 3.11; found C 53.46, H 3.41.

$(Ph_4P)[W(bdtCl_2)_3]$ (2b): A methanolic solution (10 mL) of H_2bdtCl_2 (0.07 g, 0.0003 mol) was added to WO_2Cl_2 (0.03 g, 0.0001 mol) and a purple solution was obtained after 24 h. After filtration, Ph_4PBr (0.042 g, 0.0001 mol) was added to the obtained purple solution to give deep-purple microcrystals. The precipitate was collected by filtration and dried in air. Yield: 0.07 g (61%). $C_{42}H_{26}Cl_6PS_6W$ (1150.6): calcd. C 43.84, H 2.28; found C 43.98, H 2.51.

$(C_5NH_6)[W(bdtCl_2)_3]\cdot 2CH_3OH$ (2c)·$2CH_3OH$: This complex was prepared in the same way as **2b** except that pyridinium trifluoromethanesulfonate was used instead of Ph_4PBr. Yield: 0.05 g (54%). $C_{25}H_{20}Cl_6NO_2S_6W$ (955.37): calcd. C 31.43, H 2.11, N 1.47; found C 31.59, H 2.38, N 1.51.

$(Et_4N)_2[Mo(bdtCl_2)_3]$ (3): $[MoO_2Cl_2]$ (0.04 g, 0.2 mmol) was added to a THF solution (10 mL) of H_2bdtCl_2 (0.13 g, 0.6 mmol) and the solution was stirred for 3 h. The obtained green solution was concentrated to 5 mL and purified by passing through a neutral alumina column using acetone/CH_3OH (1:4) as an eluent. A blue band was collected and concentrated to 5 mL, and addition of Et_4NI (0.05 g, 0.19 mmol) gave a blue microcrystalline powder, which was collected by filtration and dried in vacuo. Yield: 0.004 g (21%). $C_{34}H_{46}Cl_6MoNS_6$ (983.80): calcd. C 41.51, H 4.71, N 2.85; found C 41.39, H 4.65, N 2.87. UV/Vis (CH_3CN): λ_{max} (ε) = 284 nm (46800 $M^{-1}cm^{-1}$), 352 (20500), 574 (11000). CV (V vs. SCE in CH_3CN): +0.03 (reversible), +0.62 (reversible).

Calculation of θ and φ Angles (°) in Crystal Structures: The θ angle was calculated as the torsion angle between the two S atoms of $bdtCl_2$ with respect to the aligned centers of gravity between the S1, S3, and S5, and S2, S4, and S6 atoms, respectively. The φ angle was calculated as the dihedral angle between the SMS groupings of the bound ligands (S1MS2, S3MS4, S5MS6; M = Mo and W) and the trigonal planes S1S3S5 and S2S4S6, according to ref.[7] S1–S6 are labeled in Scheme S1 (see Supporting Information). Averaged values are employed in this paper. The percentage (OCT/TP) used for the OCT and TP is the average of the values θ/60 and $(90 - \varphi)/(90 - 55)$, respectively.

Other Measurements: Cyclic voltammograms were recorded at 100 mV s^{-1} with a Hokuto HZ-3000. The working and counter electrodes were a glassy-carbon disk and a platinum wire, respectively. The sample solutions were deoxygenated with a stream of N_2. The reference electrode used was an SCE. Electronic spectra were recorded with a Shimazu-U2550 spectrometer at 20 °C.

X-ray Crystallographic Study: Single crystals of **1a**, **1b**, **2a**, **2b**, and **2c** were recrystallized from acetone, hexane, acetonitrile/diethyl ether, and methanol, respectively. Although a single crystal of **3** was not obtained by recrystallization, a single crystal of **3a** was obtained by adding Et_3NHBr to a solution of **3** in CH_3CN. Each single crystal obtained was mounted on top of a glass fiber. X-ray data of the complexes were collected with graphite-monochromated Mo-K_α radiation on a Rigaku/MSC Mercury CCD diffractometer. The structures were solved by direct methods (SIR-97)[16] and expanded using DIRDIF 99.[17] The structures were refined anisotropically by full-matrix least-squares on F^2. The non-hydrogen atoms in all structures were attached at idealized positions on the carbon atoms and not refined. All structures converted in the final stages of refinement showed no movement in the atom positions. All calculations were performed with Single Crystal Structure Analysis Software, Ver. 3.6.0.[18] Further crystal data and agreement factors are listed in Tables 2 and 3.

CCDC-261315–261320 (for **1a**, **1b**, **2a**, **2b**, **2c**, and **3a**, respectively) contain the supplementary crystallographic data for this paper. These data can be obtained free of charge from The Cambridge Crystallographic Data Center via www.ccdc.cam.ac.uk/data_request/cif.

Supporting Information: Description of the θ and φ angles (Scheme S1), and detailed bond lengths [Å] and angles [°] around the metal centers (Tables S1–S6).

Table 2. Crystallographic data for **1a**, **1b**, and **3a**.

	1a	**1b**	**3a**
Formula	$C_{34}H_{46}Cl_6N_2S_6W$	$C_{66}H_{46}Cl_6P_2S_6W$	$C_{30}H_{38}Cl_6N_2MoS_6$
Molecular mass	1071.68	1489.96	927.66
Temp. [°C]	–130	–150	–150
Crystal system	orthorhombic	orthorhombic	orthorhombic
Space group	$P2_12_12_1$	$Fdd2$	$P2_12_12_1$
a [Å]	14.580(2)	24.051(1)	14.363(3)
b [Å]	15.283(2)	32.358(2)	15.971(5)
c [Å]	19.227(2)	15.3131(9)	16.641(4)
α [°]	90	90	90
β [°]	90	90	90
γ [°]	90	90	90
V [Å^3]	4284.3(8)	11917.2(12)	3799.0(17)
Z	4	8	4
$D_{calcd.}$ [g cm^{-3}]	1.661	1.660	1.622
Unique data	9244	8320	2743
Observed data	5908	7321	2310
R [%]	7.5	4.0	8.1
wR [%]	17.2	9.8	21.9
GOF	1.062	1.00	1.084

Table 3. Crystallographic data for **2a**–**2c**.

	2a	**2b**	**2c**
Formula	$C_{26}H_{26}Cl_6NS_6W$	$C_{39}H_{42}Cl_6PS_6W$	$C_{25}H_{20}Cl_6NS_6W$
Molecular mass	941.43	1135.67	955.37
Temp. [°C]	–120	–160	–160
Crystal system	monoclinic	monoclinic	monoclinic
Space group	$C2/c$	$P2_1/c$	$P2_1/n$
a [Å]	17.15(8)	22.850(2)	10.391(5)
b [Å]	19.31(8)	13.6306(9)	20.941(10)
c [Å]	20.22(10)	27.388(2)	15.497(8)
α [°]	90	90	90
β [°]	92.57(8)	94.297(4)	106.349(6)
γ [°]	90	90	90
V [Å^3]	6688.1(52)	8506.4(11)	3235.9(27)
Z	8	4	4
$D_{calcd.}$ [g cm^{-3}]	1.870	1.766	1.961
Unique data	7564	23578	7383
Observed data	5893	10962	4491
R [%]	7.2	4.9	6.5
wR [%]	19.2	12.7	14.7
GOF	1.346	0.931	0.992

Acknowledgments

This work was partly supported by a Grant for Scientific Research (no. 16750052 to H.S.) from the Japan Society for Promotion of Science and by CREST of the Japan Science and Technology Agency (JST).

[1] C. Faulmann, P. Cassoux, *Progress in Inorganic Chemistry: Solid-State Properties (Electronic, Magnetic, Optical) of Dithiolene Complex-Based Compounds* (Ed.: E. I. Stiefel), John Wiley & Sons, New Jersey, **2004**, *52*, 399–489.
[2] S. D. Cummings, R. Eisenberg, *Progress in Inorganic Chemistry: Luminescence and Photochemistry of Metal Dithiolene Complexes* (Ed.: E. I. Stiefel), John Wiley & Sons, New Jersey, **2004**, *52*, 315–367.
[3] S. J. N. Burgmayer, *Progress in Inorganic Chemistry: Dithiolene in Biology* (Ed.: E. I. Stiefel), John Wiley & Sons, New Jersey, **2004**, *52*, 491–537.
[4] J. McMaster, J. M. Tunney, C. D. Garner, *Progress in Inorganic Chemistry: Chemical Analogs of the Catalytic Centers of Molybdenum and Tungsten Dithiolene Containing Enzymes* (Ed.: E. I. Stiefel), John Wiley & Sons, New Jersey, **2004**, *52*, 539–583.
[5] J. A. McCleverty, *Prog. Inorg. Chem.* **1968**, *10*, 49–221.
[6] A. Davison, R. H. Holm, *Inorg. Synth.* **1967**, *10*, 8–26.
[7] C. L. Beswick, J. M. Schulman, E. I. Stiefel, *Progress in Inorganic Chemistry: Structures and Structural Trends in Homoleptic Dithiolene Complexes* (Ed.: E. I. Stiefel), John Wiley & Sons, New Jersey, **2004**, *52*, 55–110.
[8] G. F. Brown, E. I. Stiefel, *Inorg. Chem.* **1973**, *12*, 2140–2147.
[9] D. V. Fomitchev, B. S. Lim, R. H. Holm, *Inorg. Chem.* **2001**, *40*, 645–654.
[10] F. Knoch, D. Sellmann, W. Kem, *Z. Kristallogr.* **1993**, *250*, 300–302.
[11] C. Lorber, J. P. Donahue, C. A. Goddard, E. Nordlander, R. H. Holm, *J. Am. Chem. Soc.* **1998**, *120*, 8102–8112.
[12] B. S. Lim, J. P. Donahue, R. H. Holm, *Inorg. Chem.* **2000**, *39*, 263–273.
[13] T. E. Burrow, R. H. Morris, A. Hills, D. L. Hughes, R. L. Richards, *Acta Crystallogr., Sect. C* **1993**, *49*, 1591–1594.
[14] H. Huynh, T. Lugger, F. E. Hahn, *Eur. J. Inorg. Chem.* **2002**, 3007–3009.
[15] C. A. Goddard, R. H. Holm, *Inorg. Chem.* **1999**, *38*, 5389–5398.
[16] A. Altomare, M. Burla, M. Camalli, G. Cascarano, C. Giacovazzo, A. Guagliardi, A. Moliterni, G. Polidori, R. Spagna, *J. Appl. Crystallogr.* **1999**, *32*, 115–119.
[17] P. T. Beurskens, G. Admiraal, G. Beurskens, W. P. Bosman, R. de Gelder, R. Israel, J. M. M. Smits, **1999**. *The DIRDIF-99 program system*, Technical Report of the Crystallography Laboratory, University of Nijmegen, The Netherlands.
[18] *Crystal Structure Analysis Package*, Rigaku and Rigaku/MSC, **2000**–**2004**, 9009 New Trails Dr., The Woodlands, TX 77381, USA.

Received January 24, 2005
Published Online: June 28, 2005

